

CONTINUUM-BASED MODELLING OF RECYCLED AGGREGATE CONCRETE

Marianela Ripani^a, Sonia M. Vrech^b, Antonio Caggiano^{a,c} and Guillermo Etse^{a,b}

^a*LMNI, Intecin/CONICET, FIUBA, Materials and Structures Laboratory, Faculty of Engineering, University of Buenos Aires, Argentina. mripani@fi.uba.ar*

^b*CEMNCI, CONICET, Center for Numerical and Computational Methods in Engineering, Faculty of Exact Sciences and Technology, National University of Tucuman, Argentina. svrech@herrera.unt.edu.ar; getse@herrera.unt.edu.ar*

^c*Department of Civil Engineering, Faculty of Engineering, University of Salerno, Fisciano (SA), Italy. ancaggiano@unisa.it*

Keywords: Recycled aggregate concretes, fracture energy, gradient theory.

Abstract. The increasing use of Recycled Aggregate Concretes (RACs) in the last years due to the adverse environmental impact caused by manufacturing processes in the construction sector, makes imperative the formulation of theoretical and numerical constitutive models to effectively predict the mechanical behavior of materials and structures, to characterize the brittle or ductile failure modes at different loading regimes of such new buildings. In this work a thermodynamically consistent non-local gradient and fracture energy-based plasticity theory applicable to standard concrete at the final hardened state is extended to simulate the mechanical behavior of concretes with variable content of recycled aggregates. The predictive capabilities of the proposed constitutive formulation for RACs are verified against experimental results of tests performed at the Materials and Structures Laboratory of the University of Salerno. Both the experimental results and the theoretical formulations proposed in this paper stem out from the interuniversity collaboration developed within the framework of the European Project EnCoR (www.encore-fp7.unisa.it).

1 INTRODUCTION

The construction sector is characterized by a considerable demand for energy and raw materials. It is estimated that the greenhouse gas emissions corresponding to the construction industry represent about ten percent of the total and the half corresponds to the cement production. The design of integrated recycling processes aimed at reducing wastes and producing new "eco-friendly" materials becomes of particular interest to enhance the sustainability of the construction sector [Proske et al. \(2013\)](#).

The increasing use of recycled aggregate concretes in the last years makes imperative the formulation of theoretical and numerical constitutive models to effectively predict the mechanical behaviour of novel green materials and structures, as well as characterize the brittle or ductile failure modes at different loading regimes. For this purpose and to accurately reproduce the entire spectrum of possible failure modes (i.e. the continuous transition from brittle to ductile failure behavior), different theoretical frameworks need to be combined within one single formulation. Within the framework of the Smearred Crack Approach (SCA), brittle materials require dissipative formulations based on fracture mechanics concepts ([Bazant and Oh \(1983\)](#), [Etse and Willam \(1994\)](#), [Carpinteri et al. \(1997\)](#), [Comi and Perego \(2001\)](#), [Duan et al. \(2007\)](#), [Meschke and Dumstorff \(2007\)](#)). On the other hand, the simulation of mechanical degradation processes of ductile materials require non-local theories which appropriately and objectively describe the development of shear bands during loading processes beyond their limit strengths. In this framework, it can be taken as reference, a.o., the works by [Belytschko and Lasry \(1989\)](#), [Vardoulakis and Aifantis \(1991\)](#), [Svedberg and Runesson \(1997\)](#), [Simone et al. \(2003\)](#), [Chen et al. \(2004\)](#), [Peerlings et al. \(2004\)](#), [Vrech and Etse \(2007\)](#), [Vrech and Etse \(2009\)](#), [Vrech and Etse \(2012\)](#).

In this work the thermodynamically consistent non-local gradient and fracture energy-based Leon-Drucker Prager constitutive theory, originally formulated for natural concretes in [Vrech and Etse \(2009\)](#), is now extended to simulate the mechanical behaviour of concretes with variable content of recycled aggregates. This model is based on non-local gradient and fracture energy-based concepts and follows the thermodynamically consistent gradient plasticity theory by [Svedberg and Runesson \(1997\)](#).

The predictive capabilities of the proposed constitutive formulation for RACs are verified against experimental results corresponding to different relevant stress states, especially under compressive regime, performed at the Laboratory of Materials testing and Structures of the University of Salerno, already published by [Lima et al. \(2013\)](#).

2 LEON-DRUCKER PRAGER STRENGTH CRITERION FOR CONCRETE

The maximum strength criterion of the proposed constitutive model is obtained by combining the parabolic description of the compressive meridian by [Leon \(1935\)](#), with the Drucker-Prager circular deviatoric shape. The equation of the so-called Leon Ducker Prager (LDP) criterion for concrete is

$$F(p^*, \rho^*) = \frac{3}{2}\rho^{*2} + m_0 \left(\frac{\rho^*}{\sqrt{6}} + p^* \right) - c_0 = 0 \quad (1)$$

expressed in terms of the normalized first and second Haigh-Westergaard stress coordinates

$$p^* = \frac{I_1}{3f'_c} \quad ; \quad \rho^* = \frac{\sqrt{2J_2}}{f'_c} \quad (2)$$

being f'_c the uniaxial compressive strength and I_1 and J_2 the first and second invariants of the stress and deviatoric stress tensors, respectively. The calibration of the cohesive and frictional parameters c_0 and m_0 in terms of f'_c and the uniaxial tensile strength f'_t , leads to the following relationships

$$c_0 = 1 \quad \text{and} \quad m_0 = \frac{3(f_c'^2 - f_t'^2)}{2f_c'f_t'} \quad (3)$$

2.1 Yield surfaces of the LDP

The yield surfaces of the proposed model in the hardening and softening regimes are encompassed by one single equation as follows

$$F(p^*, \rho^*, K_h, K_s) = \frac{3}{2}\rho^{*2} + m_0 \left(\frac{\rho^*}{\sqrt{6}} + p^* \right) - K_h K_s = 0 \quad (4)$$

being K_h and K_s the hardening and softening dissipative stresses, respectively.

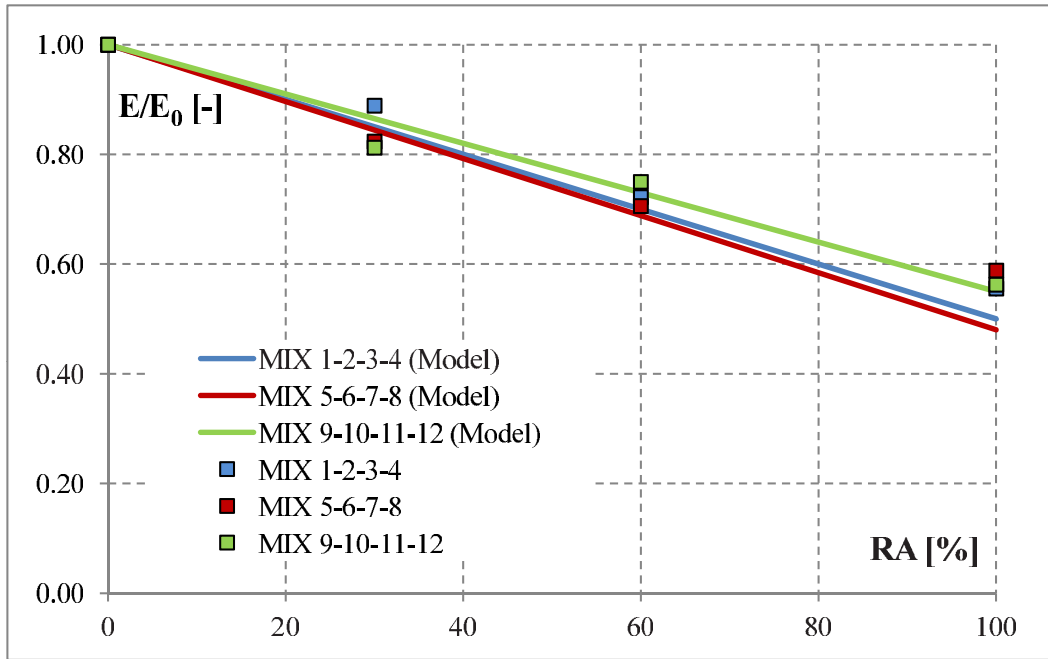


Figure 1: Decreasing elasticity modules for variable R_A .

2.2 Plastic potential

A non-associated plastic flow is adopted to accurately describe the inelastic volumetric concrete behaviour. The plastic potential corresponding to the LDP model is based on a volumetric modification of the yield condition

$$Q = F(p^*, \rho^*, K_h, K_s) + m_0 p^* (\eta - 1) = 0 \quad (5)$$

being η the non-associativity (hydrostatic) parameter that varies between $0 \leq \eta \leq 1$. The case of $\eta = 0$ corresponds to the plastic flow without dilatancy while $\eta = 1$ results in the associated flow rule.

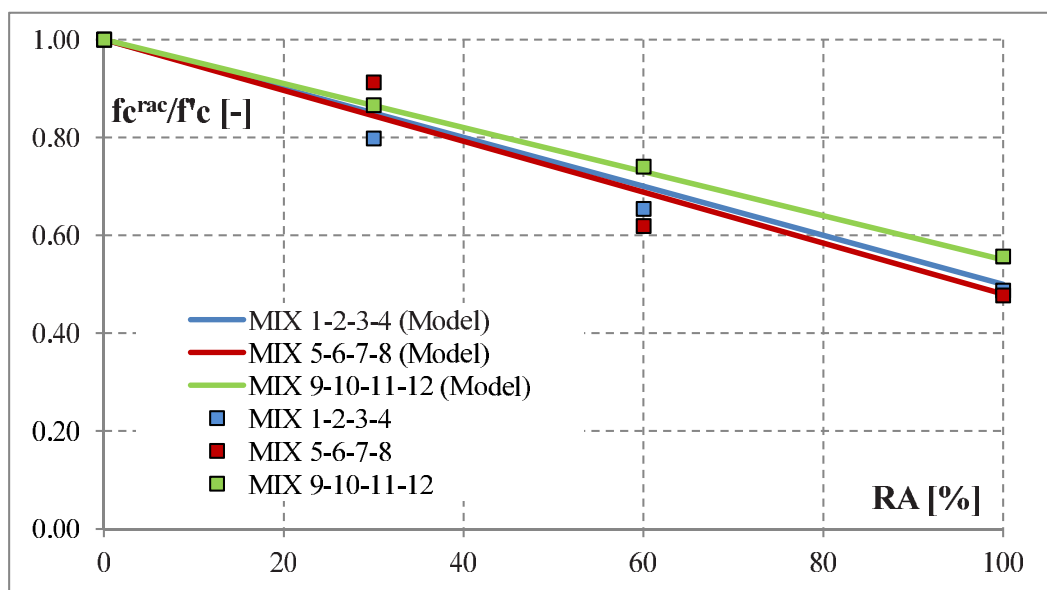


Figure 2: Uniaxial compressive strengths for variable R_A .

2.3 Pre-peak hardening regime

The post-elastic response is controlled through the evolution of the hardening dissipative stresses defined as

$$K_h = K_h^0 + 0.9 \sin \left(\frac{\pi \varepsilon_h}{2 x_h} \right) \quad (6)$$

being K_h^0 its initial value and ε_h the equivalent plastic strain computed as

$$\varepsilon_h = \|\mathbf{m}\| \lambda \quad , \quad \|\mathbf{m}\| = \left(\frac{\partial Q}{\partial \boldsymbol{\sigma}} : \frac{\partial Q}{\partial \boldsymbol{\sigma}} \right)^{1/2} \quad (7)$$

where λ represents the plastic parameter and \mathbf{m} the gradient tensor of the plastic potential. Then, x_h is the hardening ductility parameter defined in terms of the normalized confining pressure p^* as

$$x_h = A_h \exp(B_h p^*) \quad (8)$$

being A_h and B_h internal parameters to be calibrated by means of triaxial compression tests under low and high confinement.

2.4 Post-peak softening regime

Softening behavior of quasi-brittle materials like concrete is related to deformation processes under increasing inhomogeneities. The evolution and size of these heterogeneities, which define the characteristic length of the zone where the energy dissipation takes place, strongly depends on the particular boundary value problem and, therefore, cannot be treated as a material property.

In the present formulation, the instantaneous concrete strength in softening regime is obtained by means of a parallel mechanism between two components: (i) the first one directly connected with the development of micro- or macro-fracture processes, and (ii) the second one related to the damage processes in the material zones located in between active cracks.

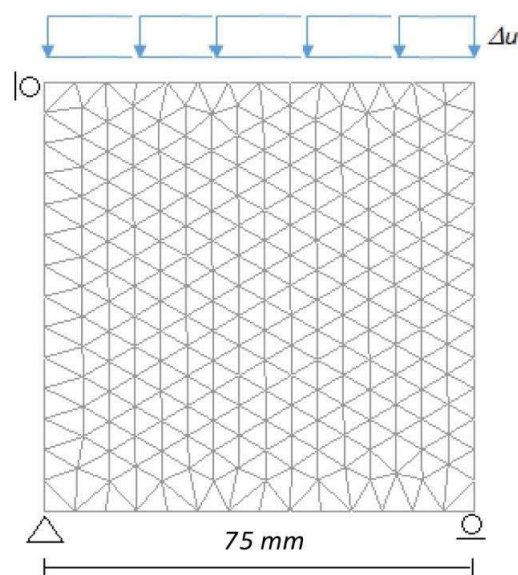


Figure 3: FE-discretization and boundary conditions for numerical compression tests

The considered mechanism controlling the strength degradation process in the post-peak regime can be mathematically expressed in terms of the dissipative stress in softening K_s and the thermodynamically consistent state variable κ_s (coincident with the plastic parameter λ). Particularly, the following relationship is considered

$$K_s(\kappa_s, \nabla \kappa_s) = K_{sf}(\kappa_s) + K_{sc}(\nabla \kappa_s) \quad (9)$$

being K_{sf} the local or fracture energy-based dissipative stress and K_{sc} the non-local gradient one. A thorough and detailed description of the softening formulation can be found in [Vrech and Etse \(2009\)](#) and is herein omitted for the sake of brevity.

3 LDP CONSTITUTIVE MODEL EXTENDED TO RAC

The original LDP model formulation above described is extended with the aim to predict the failure behaviour of RACs with variable content of recycled aggregates in partial to total substitution of natural ones. Recycled aggregates in concrete significantly affect the original mechanical properties at both fresh and hardened state. Regarding the hardened state, the characteristic mechanical behaviour observed during the experimental programs performed at the Laboratory of Materials testing and Structures of the University of Salerno, considering variable contents of coarse aggregate replacements (30%, 60% and 100%) demonstrate that the replacement of natural aggregates with recycled ones affects in first place the uniaxial compressive strength, an essential property of concrete at hardened state. Another essential feature is the reduction of pre and post-peak ductility with increasing RA content. Regarding these typical properties, the extended LDP model must be able to numerically reproduce RACs failure and its mechanical behaviour.

3.1 Elastic regime

According to [Corinaldesi and Moriconi \(2009\)](#) experimental data, Young moduli of RACs are generally lower than those of NACs. The RAC elasticity modulus values E , deduced from

experimental programs performed on uniaxial compression tests (Lima et al. (2013)), considering variable contents of aggregate replacements ((0%, 30%, 60% and 100%) and normalized respect to the corresponding NAC value E_0 , are summarized in Fig. 1. Based on this, the following approximation is proposed to mathematically estimate the degraded RAC elasticity modules as a function of E_0

$$E = (1 - \gamma)E_0 \quad \text{with} \quad \gamma = 0.005R_A \quad (10)$$

being γ the damage induced by R_A , the substitution percentage which varies from 0 to 100 and γ the damage induced by the R_A content.

Mixes	FA [%]	RA [%]	f_c^{rac} [MPa]	f_t^{rac} [MPa]	E [MPa]
1-2-3-4	32	0	41.05	5.34	36000
		30	32.76	4.26	32000
		60	26.86	3.49	26000
		100	12.19	1.58	20000
5-6-7-8	88	0	42.61	5.54	34000
		30	38.89	5.06	28000
		60	26.38	3.04	24000
		100	20.33	2.64	20000
9-10-11-12	128	0	35.47.61	4.61	32000
		30	30.72	3.99	26000
		60	26.27	3.42	24000
		100	19.76	2.57	18000

Table 1: Mixes properties.

ν	Poisson coefficient	0.20
η	Non-associativity coefficient	0.12
A_h	Hardening law	0.0007
B_h	Hardening law	-0.019
C_f	Local softening law	50.00
D_f	Local softening law	51.00
E_c	Gradient softening law	0.50
F_c	Gradient softening law	2.00
u_r	Maximum crack opening in Mode I	0.127 mm
h_t	NAC fracture characteristic length	70.00 mm
l_{cm}	Maximum gradient characteristic length	70.00 mm
l_{ca}	Maximum aggregate size	18.00 mm
H_{sc}	Gradient softening parameter	1.00 MPa

Table 2: Calibrated internal parameters.

3.2 Strength criterion for RAC

The following linear law is employed to mathematically estimate the degraded RAC uniaxial compressive strength f_c^{rac} , as a function of R_A

$$f_c^{rac} = (1 - \gamma)f_c' \quad \text{with} \quad \gamma = 0.005R_A \quad . \quad (11)$$

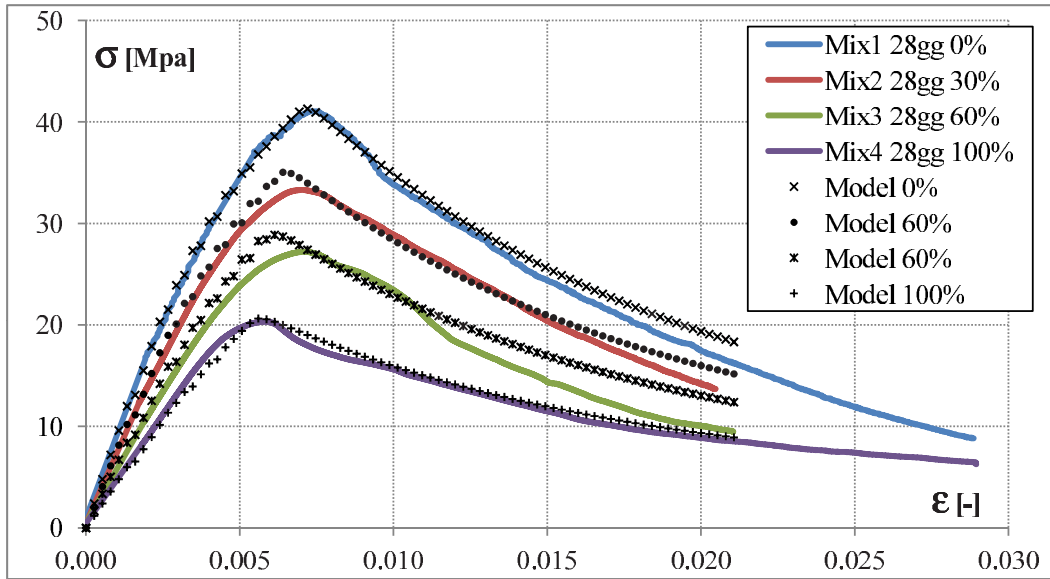


Figure 4: Uniaxial compression test: Mixes 1 to 4.

The resulting linear trend of normalized uniaxial compressive strengths of RACs is shown in Fig. 2. In the same way, it can be set for the uniaxial tensile strength the linear approximation law

$$f_t^{rac} = (1 - \gamma)f_t' \quad (12)$$

Based on the eqs. (11) and (12) it follows that the cohesive and frictional parameters c_0 and m_0 of eq. (3) become

$$c_0 = 1 \quad \text{and} \quad m_0 = \frac{3(f_c^{rac2} - f_t^{rac2})}{2 f_c^{rac} f_t^{rac}} \quad (13)$$

3.3 Hardening/softening modifications of the LDP model extended to RAC

In pre-peak regime, the observed hardening response is almost unaffected by the presence of RAs substituting the natural ones and then, the same formulation adopted for NAC can be used.

Contrarily, the softening behavior of RAC is mainly affected by the presence of RA. Such a response is controlled through the softening formulation described in Subsection 2.4. The considered dissipative stress in softening K_s is computed as the additive contribution of a local (fracture energy-based) dissipative stress K_{sf} and a non-local gradient one K_{sc} . The local softening dissipative stress is calculated as

$$K_{sc} = \exp\left(-5 \frac{h_f}{u_r} \varepsilon_f\right) \quad , \quad \varepsilon_f = \|\langle \mathbf{m} \rangle\| \lambda \quad (14)$$

in terms of the fracture characteristic length h_f , which defines the distance between cracks while u_r represents the maximum crack opening displacement in mode I. In quasi-brittle materials like concrete the distance between microcracks strongly depends on the type of fracture as well as on the acting confining pressure. Particularly, in mode I type of fracture no confining pressure exists and the microcracks lead to one single macrocrack. It follows that the fracture energy-based characteristic length approaches its maximum value (the specimen high h_t): i.e., $h_f =$

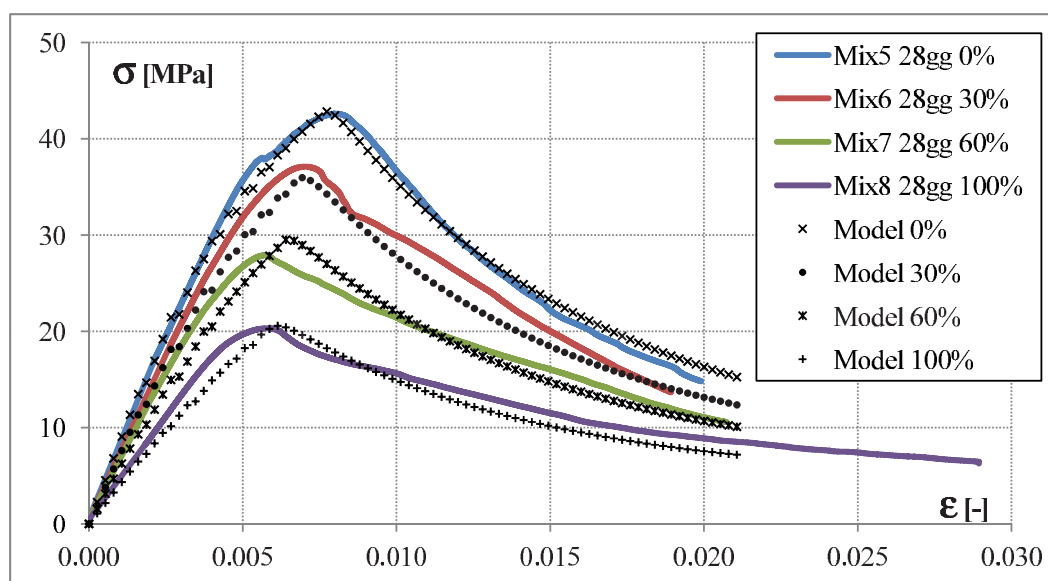


Figure 5: Uniaxial compression test: Mixes 5 to 8.

h_t . With increasing confining pressure under mode II type of failure the microcrack density increases and h_f tends to 0.

The present formulation oriented to RACs, considers that the variation of the fracture energy-based characteristic length from its maximum possible value h_t^{rac} is controlled by means of the normalized pressure-dependent function $R_f(p^*)$

$$h_f(p^*) = \frac{h_t^{rac}}{R_G(p^*)}; \quad R_G(p^*) = \begin{cases} 1, & p^* \geq 0 \\ C_f + D_f \sin\left(2p^* - \frac{\pi}{2}\right), & -1.5 \leq p^* < 0 \\ 100, & p^* < -1.5 \end{cases} \quad (15)$$

being C_f and D_f softening material parameters to be calibrated. The maximum value of the fracture energy-based characteristic length for RACs h_t^{rac} is calibrated by means of uniaxial compression tests for variable contents of RA. The following non-linear relationship between h_t^{rac} and h_t is established in terms of R_A for all mixes

$$h_t^{rac} = C_h h_t \quad \text{with} \quad C_h = 1 - \gamma^2 \quad . \quad (16)$$

The non-local gradient dissipative stress K_{sc} can be computed according to [Vrech and Etse \(2009\)](#).

4 NUMERICAL RESULTS AND COMPARISONS

In this section, the predictive capabilities of the proposed constitutive model to reproduce the mechanical behaviour of RACs with variable content of recycled aggregates in partial to total substitution of natural ones are verified. The attention focuses on the numerical simulation of experimental tests performed on RAC cubic specimens of $150 \times 150 \times 150 \text{ mm}^3$ loaded under uniaxial compression ([Lima et al., 2013](#)). These experimental results are assumed as benchmark for validating the proposed numerical simulations. In the present analysis a dual-mixed finite element formulation proposed by [Svedberg \(1999\)](#) is considered. The axysymmetrical panel adopting the constant strain triangle (CST) elemental discretization and the adopted uniform

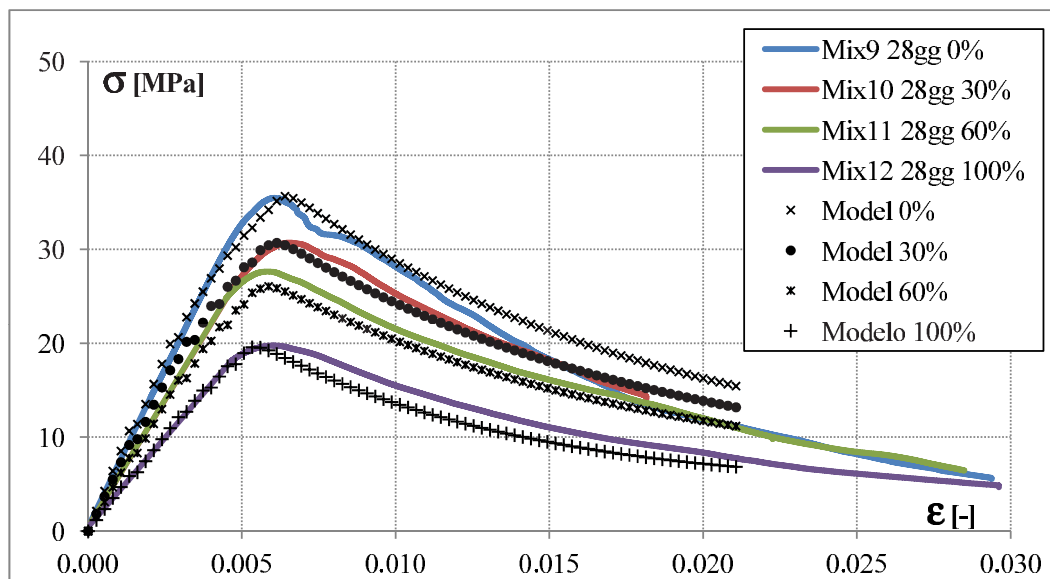


Figure 6: Uniaxial compression test: Mixes 9 to 12.

boundary conditions are schematized in Fig. 3. Due to the double symmetry of the problem, the FE discretization covers only one quarter of the concrete panel. Then, the compressive loads on the top of the FE mesh are introduced by means of uniform vertical nodal displacements. Material properties corresponding to the tested mixes are detailed in Table 1. The experimental specimens are also composed by three different concrete types, characterized by variable Fly-Ash (FA) percentages (32%, 88% and 128% as highlighted in Table 3) and different fractions of recycled aggregates (0%, 30%, 60% and 100%, see Table 1). General internal parameters adopted for these numerical analysis are summarized in Table 2.

Comparisons between experimental and numerical results in terms of axial stresses vs. axial strains for uniaxial compression tests are highlighted in Fig. 4 to 6. Particularly, those figures compare experimental results against numerical ones corresponding to Mixes 1-4, 5-8 and 9-12, respectively. From the numerical point of view, the presented results demonstrate the predictive capabilities of the fracture energy and gradient plasticity-based LDP model to reproduce the mechanical behavior of RACs under the uniaxial compression test and considering a wide range of concrete mixes. The decreasing uniaxial compressive strength with increasing volume fractions of RA is well reproduced in all the analyzed mixes. Moreover, good agreements between experimental and numerical results can be observed for initial elastic, hardening and softening regimes. The reduction of pre- and post-peak ductility with increasing RA content is also predicted.

5 CONCLUSIONS

The thermodynamically consistent gradient and fracture energy-based Leon - Drucker Prager constitutive model for quasi-brittle materials has been extended to predict the mechanical response of RACs with variable amounts of RA in partial to total substitution of natural ones. The damage induced by RA content coefficient was introduced to take into account the reduction of the fundamental properties when increasing values of RA percentages are considered. Internal parameters involved in hardening and softening laws were calibrated according to the experimental results performed at the Materials and Structural Testing Laboratory of the University

Mix	C kg/m^3	FA kg/m^3	RA %	w kg/m^3	w_{add} kg/m^3	NA ₃	NA ₂	NA ₁	Sand	RA ₃	RA ₂	RA ₁	Sand
1	250	80	0	150	14.02	505	470	165	750	-	-	-	-
2	250	80	30	150	21.86	-	408	165	750	445	55	-	-
3	250	80	60	150	38.16	-	-	-	750	445	415	145	-
4	250	80	100	150	109.65	-	-	-	-	445	415	145	660
5	250	220	0	150	11.28	545	490	170	500	-	-	-	-
6	250	220	30	150	17.85	35	490	170	500	450	-	-	-
7	250	220	60	150	28.99	-	-	185	500	455	450	-	-
8	250	220	100	150	98.84	-	-	-	-	400	375	130	595
9	200	255	0	150	11.28	545	490	170	500	-	-	-	-
10	200	255	30	150	17.85	35	490	170	500	450	-	-	-
11	200	255	60	150	28.68	-	-	175	500	455	445	-	-
12	200	255	100	150	98.84	-	-	-	-	400	375	130	595

Table 3: Proportions of mix components.

of Salerno. Numerical analysis based on the proposed model was performed for uniaxial compressions tests. The comparison between these results against the experimental ones highlights the predictive potential of the proposed formulation.

6 ACKNOWLEDGMENT

The authors acknowledge the financial support for this work by CONICET (Argentinean National Council for Science and Technology) through the Grant PIP 112-200801-00707 and CIUNT (Research council of the National University of Tucuman) through the Grant 26/E479. The support to networking activities provided by *ŞEncore* Project (FP7-PEOPLE-2011- IRSES n 295283; <http://www.encore-fp7.unisa.it/>) funded by the European Union within the Seventh Framework Programme is also gratefully acknowledged by the authors.

7 APPENDIX: CONSIDERED EXPERIMENTAL TESTS

The constitutive formulation developed in this work has been validated through experimental data of a wide experimental campaign carried out on concretes composed by RA and Fly-Ash (FA) in partial substitution of natural aggregates (NAs) and Cement (C) respectively, conducted at the Materials and Structural Testing Laboratory of the University of Salerno and reported by Lima et al. (2013).

Table 3 describes the composition of such mixes. Particularly, the first column of the table denotes the different mixes, C and FA the content of cement and fly-ash respectively, in kg/m^3 . RA provides the percentage of recycled aggregates [%]. w and w_{add} deal with the available water for the chemical reaction and the "extra" quantity depending on the water absorption capacity of the employed aggregates, respectively, measured in kg/m^3 . Four fractions characterize both NA and RA in kg/m^3 : i.e. NA₃, NA₂, NA₁, RA₃, RA₂, RA₁ and sand.

REFERENCES

- Bazant Z. and Oh B. Crack band theory for fracture of concrete. *Materials and Structures*, 16:155–177, 1983.
- Belytschko T. and Lasry D. A study of localization limiters for strain-softening in statics and dynamics. *Computers and Structures*, 33:707–715, 1989.

- Carpinteri A., Chiaia B., and Nemati K. Complex fracture energy dissipation in concrete under different loading conditions. *Mechanics of Materials*, 26:93–108, 1997.
- Chen J., Zhang X., and Belytschko T. An implicit gradient model by a reproducing kernel strain regularization in strain localization problems. *Computer Methods in Applied Mechanics and Engineering*, 193:2827–2844, 2004.
- Comi C. and Perego U. Fracture energy based bi-dissipative damage model for concrete. *International Journal of Solids and Structures*, 38:6427–6454, 2001.
- Corinaldesi V. and Moriconi G. Influence of mineral additions on the performance of 100% recycled aggregate concrete. *Construction and Building Materials*, 23:2869–2876, 2009.
- Duan K., Hu K., and Wittmann F. Size effect on specific fracture energy of concrete. *Engineering Fracture Mechanics*, 74:87–96, 2007.
- Etse G. and Willam K. A fracture energy-based constitutive theory for inelastic behavior of plain concrete. *Journal of Engineering Mechanics*, 120:1983–2011, 1994.
- Leon A. Ueber das Mass der Anstrengung bei Beton. *Ingenieur Archiv*, 4:421–431, 1935.
- Lima C., Caggiano A., Faella C., Martinelli E., Pepe M., and Realfonzo R. Physical properties and mechanical behaviour of concrete made with recycled aggregates and fly-ash. *Construction and Building Materials*, 47:547–559, 2013.
- Meschke G. and Dumstorff P. Energy-based modeling of cohesive and cohesionless cracks via X-FEM. *Computer Methods in Applied Mechanics and Engineering*, 196:2338–2357, 2007.
- Peerlings R., Massart T., and Geers M. A thermodynamically motivated implicit gradient damage framework and its application to brick masonry cracking. *Computer Methods in Applied Mechanics and Engineering*, 193:3403–3417, 2004.
- Proske T., Hainer S., Rezvani M., and Graubner C. Eco-friendly concretes with reduced water and cement contents - Mix design principles and laboratory tests. *Cement and Concrete Research*, 51:38–46, 2013.
- Simone A., Wells G., and Sluys L. From continuous to discontinuous failure in a gradient-enhanced continuum damage model. *Computer Methods in Applied Mechanics and Engineering*, 192:4581–4607, 2003.
- Svedberg T. *On the modelling and numeric of gradient-regularized plasticity coupled damage*. Phd. Thesis, Chalmers University of Technology, Sweden, 1999.
- Svedberg T. and Runesson K. A thermodynamically consistent theory of gradient-regularized plasticity coupled to damage. 13:669–696, 1997.
- Vardoulakis I. and Aifantis E. A gradient flow theory of plasticity for granular materials. *Acta Mechanica*, 87:197–217, 1991.
- Vrech S. and Etse G. FE approach for thermodynamically consistent gradient-dependent plasticity. *Latin American Applied Research*, 37:127–132, 2007.
- Vrech S. and Etse G. Gradient and fracture energy-based plasticity theory for quasi-brittle materials like concrete. *Computer Methods in Applied Mechanics and Engineering*, 199:136–147, 2009.
- Vrech S. and Etse G. Discontinuous bifurcation analysis in fracture energy-based gradient plasticity for concrete. *International Journal of Solids and Structures*, 49:1294–1303, 2012.